

Communication

Enantioselective Epoxidation by Flavoprotein Monooxygenases Supported by Organic Solvents

Daniel Eggerichs ¹, Carolin Mügge ¹ , Julia Mayweg ¹, Ulf-Peter Apfel ^{2,3}  and Dirk Tischler ^{1,*} 

¹ Microbial Biotechnology, Faculty of Biology and Biotechnology, Ruhr-Universität Bochum, Universitätsstr. 150, 44780 Bochum, Germany; daniel.eggerichs@rub.de (D.E.); carolin.muegge@rub.de (C.M.); julia.mayweg@gmail.com (J.M.)

² Activation of Small Molecules, Faculty of Chemistry and Biochemistry, Ruhr-Universität Bochum, Universitätsstr. 150, 44780 Bochum, Germany; ulf.apfel@rub.de

³ Fraunhofer UMSICHT, Division of Energy, Osterfelder Strasse 3, 46047 Oberhausen, Germany

* Correspondence: dirk.tischler@rub.de; Tel.: +49-234-32-22656

Received: 29 April 2020; Accepted: 14 May 2020; Published: 19 May 2020



Abstract: Styrene and indole monooxygenases (SMO and IMO) are two-component flavoprotein monooxygenases composed of a nicotinamide adenine dinucleotide (NADH)-dependent flavin adenine dinucleotide (FAD)-reductase (StyB or IndB) and a monooxygenase (StyA or IndA). The latter uses reduced FAD to activate oxygen and to oxygenate the substrate while releasing water. We circumvented the need for the reductase by direct FAD reduction in solution using the NAD(P)H-mimic 1-benzyl-1,4-dihydronicotinamide (BNAH) to fuel monooxygenases without NADH requirement. Herein, we report on the hitherto unknown solvent tolerance for the indole monooxygenase from *Gemmobacter nectariphilus* DSM15620 (*GnIndA*) and the styrene monooxygenase from *Gordonia rubripertincta* CWB2 (*GrStyA*). These enzymes were shown to convert bulky and rather hydrophobic styrene derivatives in the presence of organic cosolvents. Subsequently, BNAH-driven biotransformation was furthermore optimized with regard to the applied cosolvent and its concentration as well as FAD and BNAH concentration. We herein demonstrate that *GnIndA* and *GrStyA* enable selective epoxidations of allylic double bonds (up to 217 mU mg^{−1}) in the presence of organic solvents such as tetrahydrofuran, acetonitrile, or several alcohols. Notably, *GnIndA* was found to resist methanol concentrations up to 25 vol.%. Furthermore, a diverse substrate preference was determined for both enzymes, making their distinct use very interesting. In general, our results seem representative for many IMOs as was corroborated by in silico mutagenetic studies.

Keywords: styrene monooxygenase; indole monooxygenase; two-component system; chiral biocatalyst; solvent tolerance; biotransformation; epoxidation; NAD(P)H-mimics

1. Introduction

Styrene and indole monooxygenases (StyA or IndA) are the initial enzymes in degradation pathways of human-made aromatic pollutants, such as styrenes, within several bacteria [1–3]. Similar to the general detoxification pathways in higher organisms, hydrophobic compounds are typically oxidized in bacteria to increase their water solubility and create a functional moiety, which can be easily metabolized by downstream enzymes [4,5]. For example, styrene monooxygenases perform the oxidation of double bonds with molecular oxygen and an additional reduction equivalent to form an epoxide along with water as side product [6,7].

Due to their role as mainly detoxifying enzymes, SMOs and IMOs accept a large variety of substrates. Although the highest activities were described for conjugated double bonds in direct proximity of an

aromatic ring, SMOs were likewise shown to enable the epoxidation of unconjugated double bonds even without the aromatic moiety [8–10]. Furthermore, SMOs and IMOs catalyze sulfoxidations of artificial substrates at increased rates as compared to their supposed natural substrates [11,12].

Apart from their occurrence during biological degradation pathways, chiral epoxides are important building blocks for the industrial production of fine chemicals such as drugs or fungicides (Figure 1) [13,14]. Due to their broad substrate scope, their stability and remarkably high regio- and stereoselectivity, SMOs and IMOs are promising candidates for the industrial application toward chiral biomolecules [13,15–17]. Along this line, several studies highlighted the versatile applications for this enzyme class up to pilot scale yielding >300 g (*S*)-styrene oxide [18–20].

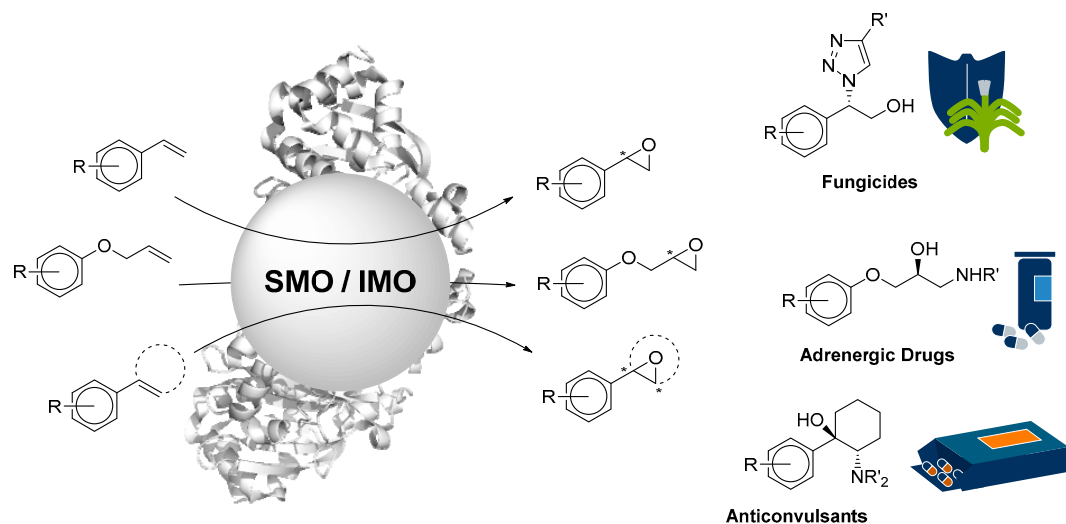


Figure 1. Styrene and indole monooxygenases activate double bonds by chiral epoxidation. Those epoxide intermediates are valuable building blocks in the chemical industry and can be further processed toward fine chemicals.

Nevertheless, there are some significant drawbacks that have to be overcome before SMOs or IMOs can be used on an even larger industrial scale. First, SMOs and IMOs depend on a suitable electron donor to reduce their flavin adenine dinucleotide (FAD) cofactor after each reaction cycle. In nature, nicotinamide adenine dinucleotide (NADH) is consumed stoichiometrically and regenerated *in vivo*, but it is too expensive to use with isolated enzymes on larger scales.

Among the enzyme family, SMOs and IMOs can be differentiated into mono- and two-component systems [7,21]. The first contain a NADH binding domain which allows them to reduce their FAD cofactor autonomously but limits them exclusively to their natural cosubstrate. In contrast, two-component oxygenases require an additional reductase (StyB or IndB) which supplies the oxygenase with reduced FAD in nature. Furthermore, the self-sufficient mono-component enzymes of these monooxygenases show a lower oxygenase activity than the others [12,22,23].

Notably, in artificial systems, two-component enzymes can also use FADH_2 from the solution [24]. Thus, cofactor reduction by chemical methods without the need for NADH as an expensive cosubstrate is possible. Commonly, two-component SMOs and IMOs are cost-efficiently fueled by (a) the reduction of FAD by chemical agents (e.g., sodium thiosulfate or ruthenium complexes [8,25]), (b) the use of NAD(P)H-mimics [26] or (c) the electrochemical reduction of the cofactor [27].

In this study, the NAD(P)H-mimic 1-benzyl-1,4-dihydronicotinamide (BNAH) was preferred as cheap and easy to synthesize electron donor for the FAD cofactor in solution [11].

In addition to the typical need to apply expensive reductants, the limited solubility of many organic substrates in aqueous solutions (e.g., 2.9 mM for styrene) is a key problem and restricts substrate conversion to the lower millimolar range using isolated biocatalysts [28]. For higher amounts, whole cells have to be used in two-phase systems or with cosolvents [29]. In particular, styrene derivatives

with hydrophobic side chains have a comparably low water solubility [30]. In addition, only a few enzymes with uncommonly capacious substrate binding sites are known to accept those large styrene derivatives [11]. Nevertheless, chiral styrene oxide derivatives with hydrophobic side chains are important industrial precursors for several drugs (Figure 1). In this study, we maximized the production of these compounds in an overall process optimization by applying various water-miscible solvents to increase the amount of substrate in solution and make it accessible for the enzymes. Our results show remarkably high product formation in reactions catalyzed by the IMO designated as *GnIndA* from *Gemmobacter nectarophilus* DSM15620 in presence of organic solvents.

To the best of our knowledge, solvent-tolerant SMOs or IMOs have not been reported before. Herein, we describe the systematical reaction optimization toward several water-miscible cosolvents for the probable solvent-tolerant *GnIndA* and *GrStyA* from *Gordonia rubripertincta* CWB2. In addition, our work highlights criteria which will help to identify solvent-tolerant enzymes based on their sequence and allows creating more robust mutants.

2. Results

2.1. Reaction Condition Optimization

GrStyA and *GnIndA* were successfully produced by recombinant expression as described previously [11]. Both enzymes were obtained in pure form after His-tag purification using an N-terminal His₁₀-tag and yielded 15 mg L⁻¹ for *GrStyA* and 50 mg L⁻¹ for *GnIndA* (Figure S1). Since both enzymes were described to accept styrene derivatives with large side chains as substrate [11], we aimed to maximize the product amount in a BNAH-driven process.

Because *GnIndA* and *GrStyA* belong to the subgroup of two-component systems, they were expected to accept NAD(P)H-mimics and their activity was established with BNAH as reduction equivalent (standard conditions: 20 mM Tris-HCl pH 7.5, 10 mM BNAH, 50 µM FAD, 1 mM dithiothreitol, 5 vol.% glycerol, 20 U/mL catalase and 10 vol.% MeOH for *GnIndA* or 5 vol.% DMSO for *GrStyA*). Dithiothreitol was applied to support enzyme stability as reported earlier [22]. For the sake of comparability of in-house performed assays, the protocol was kept unchanged, even though adding dithiothreitol was not mandatory for herein tested enzymes (data not shown). For both enzymes, the optimal BNAH concentration was determined to be 15 mM while for *GrStyA* a comparable high product amount was also observed at a concentration of 10 mM BNAH. These concentrations are equal to a 200- to 300-fold BNAH excess toward FAD (Figure 2a). For *GnIndA*, lower product amounts with 10 mM BNAH were observed in contrast to otherwise similar values in comparison with *GrStyA*.

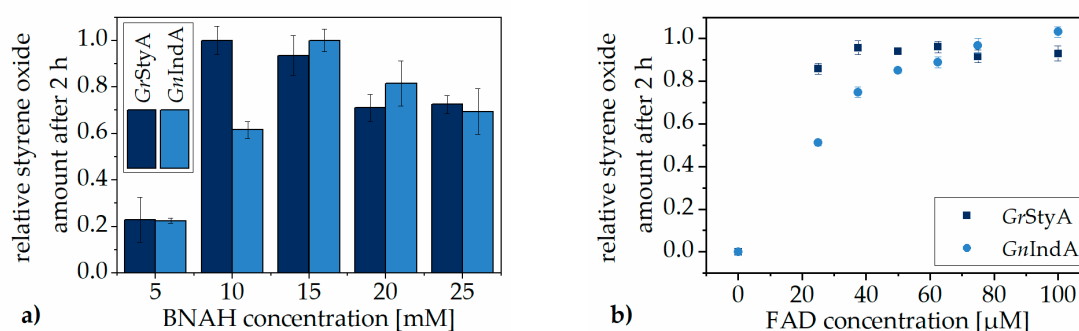


Figure 2. Relative produced styrene oxide amount under standard reaction conditions (20 mM Tris-HCl pH 7.5, 1 mM dithiothreitol, 5 vol.% glycerol, 20 U/mL catalase and 10 vol.% MeOH for *GnIndA* or 5 vol.% DMSO for *GrStyA*) in variation of (a) BNAH (50 µM FAD added) and (b) FAD concentration (10 mM BNAH added) for *GrStyA* and *GnIndA*: Both enzymes show their maximal product amount for a supplied BNAH concentration of 10 to 15 mM in presence of 50 µM FAD. The cofactor concentration to reach >90% relative product amount was determined for *GrStyA* >40 µM and for *GnIndA* > 60 µM FAD.

In addition, the FAD saturation concentration was found to be higher than for *GrStyA* (Figure 2b). *GrStyA* reached >80% of the maximal produced styrene oxide supplied with 25 μ M FAD and no further increase of product amount was observed for cofactor concentrations above 40 μ M (Figure 2b). In contrast, *GnIndA* required more than 60 μ M FAD to reach >90% of the maximal substrate production and reached the maximal product formation at a FAD concentration of 100 μ M.

These findings indicate a lower affinity of *GnIndA* toward FADH₂. The BNAH-driven FAD reduction in solution is enzyme-independent, but the uptake of reduced FADH₂ correlates with the affinity of the enzyme toward the cofactor. Since the effect of a lower affinity is only detectable under limiting conditions, different product formation rates can only be observed in low FAD concentration ranges as it was demonstrated for *GnIndA* (Figure 2).

After the optimization of cofactor and cosubstrate concentrations, we tested the influence of organic solvents on the enzymatic reaction. The cosolvent is required to increase the solubility of the anticipated substrates in this study and to make those styrene derivatives with hydrophobic side chains accessible for the biocatalyst. In addition, BNAH is also hardly soluble in aqueous solutions and likewise requires cosolvents. In total, nine water-miscible solvents with logP_{O/W} values ranging from −1.35 (dimethyl sulfoxide) to +0.46 (tetrahydrofuran) were applied to the enzymatic reaction in concentrations up to 25 vol.% (Figure 3, Table S1). In this concentration range, the dissolved amount of the most hydrophobic substrate 1-phenyl-1-cyclohexene could be increased between a factor of three (methanol) and 100 times (1-propanol). This increase marks the upper limit for effects achieved by the cosolvent regarding the substrate solubility (Figure S2). Since styrene is about 1.6 times better soluble in water by the means of the logP_{O/W} value (Table 1), a less pronounced effect in solubility increase can be expected by solvent addition for the more polar styrene. Nevertheless, the unsubstituted styrene was chosen as standard substrate to quantify the effects of each solvent and its concentration on the overall enzyme reaction. As measure of the effect, the produced amount of styrene oxide after 2 h of reaction time was used.

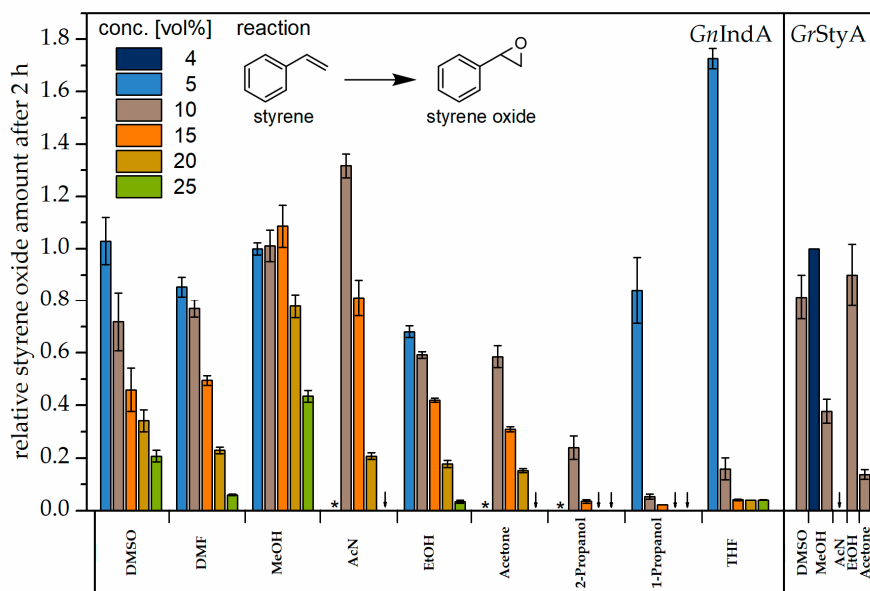
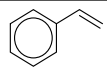
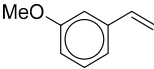
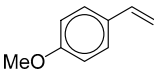
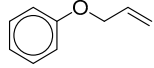
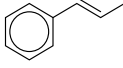
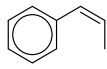
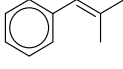
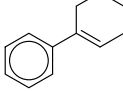
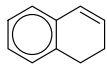


Figure 3. Relative styrene oxide amount formed by *GnIndA* (left) and *GrStyA* (right) in presence of nine organic solvents: In general, for *GnIndA* a remarkably high product formation up to 15 vol.% cosolvent was observed while MeOH and THF were outstanding due to the stable product formation at higher concentrations and the increased product formation in lower concentration ranges, respectively. Except for DMSO and EtOH, a significantly reduced product amount was detected for *GrStyA* already at 10 vol.% cosolvent. The relative styrene oxide amount is normalized to 5 vol.% MeOH (*GnIndA*, 0.70 mM styrene oxide) resp. 4 vol.% MeOH (*GrStyA*, 0.47 mM styrene oxide). * not measured.

Table 1. Conversion of different substrates by flavin-dependent monooxygenases.

Substrate	Water Solubility [30] (logP _{O/W}) [28]	Observed Activity ^a [mU mg ⁻¹] (Enantiomeric Excess)	
		<i>GrStyA</i>	<i>GnIndA</i>
 Styrene	2.85 mM (2.95)	50 ± 8 (>98% S)	212 ± 7 (>80% S)
Product Formation Rate ^b [%]			
 3-Methoxystyrene	- (2.9) ^c	81 ± 8	60 ± 2
 4-Methoxystyrene	- (3.1) ^c	<1	n.d.
 Allyl phenyl ether	- (2.94)	7 ± 1	2 ± 1
 <i>E</i> -β-Methylstyrene	1.18 mM (3.35)	88 ± 9	169 ± 3
 <i>Z</i> -β-Methylstyrene	- (3.2) ^c	137 ± 5	65 ± 11
 β,β-Dimethylstyrene	- (3.8) ^c	122 ± 3	30 ± 1
 1-Phenyl-1-cyclohexene	- (4.5) ^c	7 ± 1	<1
 1,2-Dihydronaphtalene	- (3.2) ^c	100 ± 1	n.d.

^a initial styrene oxide formation rate under optimal conditions (20 mM Tris-HCl pH 7.5, 1 mM dithiothreitol, 5 vol.% glycerol, 20 U/mL catalase and 10 vol.% MeOH for *GnIndA* or 5 vol.% DMSO for *GrStyA*), ^b initial epoxide production rate normalized to formation rate of styrene oxide (100%) under the same conditions, ^c computed values by XLogP3 3.0 (PubChem release 2019.06.18), n.d. = not detected.

This simplification allows no differentiation between the contributions of either the enzyme stability, increased activity, or the substrate accessibility in solution; it rather shows the sum of all effects and is sufficient in order to develop an efficient enzymatic process in the first place.

The obtained styrene oxide amount was normalized to the amount produced in presence of 5 vol.% (*GnIndA*) or 4 vol.% methanol (*GrStyA*) (Figure 3). For the enzymatic reaction catalyzed by *GnIndA*, a remarkably high product formation after addition of various solvents in concentrations up to 15 vol.% was found, while methanol was outstanding with still 43% product production at 25 vol.% organic solvent in solution. In presence of up to 15 vol.% acetonitrile, an increased product amount was observed in comparison to 5 vol.% MeOH and other solvents at the respective concentrations. The highest increase in product formation of +72% relative to the result in 5 vol.% MeOH was found for 5 vol.% THF, which is the solvent with the most positive logP_{O/W} value (+0.46). The detected styrene oxide amount for solvents with positive logP_{O/W} values (THF, 1- and 2-propanol) is comparably high at 5 vol.% in general, but a significant decrease in product formation can be observed for higher concentrations. It has to be highlighted that the enantiomeric excess (*ee*) was investigated for selected solvents and no variation was observed under any investigated condition (*GnIndA*: >80% (*S*)-styrene oxide; Table S2).

In contrast to *GnIndA*, a decreased product formation in presence of most of the tested solvents was observed for the same reaction catalyzed by *GrStyA*. Only for DMSO and ethanol a product amount above 80% relative to standard conditions was detected at 10 vol.% cosolvent (Figure 3).

2.2. Substrate Spectrum

After optimization of the reaction conditions, we tested the enzymatic activity of both enzymes on eight substrates which contain aliphatic residues at the vinyl chain or methoxy modifications at the aromatic ring (Table 1). For all substrates, the water solubility is equal to or up to 1.6-times lower than for the unsubstituted styrene by means of the $\log P_{O/W}$ value. In addition, all substrates exhibit a larger sterical size than styrene due to their substitution patterns. The substitutions were chosen to cover diverse positions within the molecule in order to compare the influence of variations at these positions on the enzymatic activity. Ether moieties were selected in *para*- and *meta*-position relative to and between the reactive double bond and the phenyl unit to investigate their influence on substrate recognition by the enzyme. The *E*- and *Z*-selectivity was investigated using a methyl group at the β -vinyl carbon in *E*- and *Z*- β -methylstyrene. In comparison to this small residue, a six-membered ring in 1-phenyl-1-cyclohexene and 1,2-dihydronaphthalene was selected to determine the *E*- and *Z*-selectivity as example for larger substituents.

Based on the findings described in the previous section, 10 vol.% methanol was applied as cosolvent for *GnIndA* in these experiments because it allowed the best combination of produced styrene oxide and substrate concentration in solution (Figure 3 and Figure S2). For *GrStyA*, a cosolvent concentration of 5 vol.% DMSO was chosen due to the high product formation in presence of DMSO. Furthermore, DMSO dissolved twice the substrate amount than ethanol at 5 vol.% respectively, for which also a stable product formation up to 10 vol.% was detected (Figure S2). The remaining reaction conditions were applied as described in the previous section. For the determination of product formation rates, the respective activity on styrene under optimal conditions was used as 100% value.

Our results show a four-fold higher activity of *GnIndA* on the standard substrate styrene than observed for *GrStyA*. In return, for the less active *GrStyA*, an enantiomeric excess of >98% (*S*)-styrene oxide was detected while for *GnIndA* an *ee*-value >80% (*S*)-styrene oxide was observed. Furthermore, many substrate-dependent differences in the product formation rates were found. For *GnIndA* with the higher activity for styrene oxidation, the acceptance of larger substrates is overall reduced. For most substrates, a more than 35% reduced activity was observed while no product could be detected for 4-methoxystyrene and 1,2-dihydronaphthalene. The latter is representative for all tested substrates containing a residue in *Z*-position to the aromatic ring: For all of these substrates, a reduced enzyme activity was observed. In contrast, for *E*- β -methylstyrene (observed activity $\sim 358 \text{ mU mg}^{-1}$), a $69 \pm 3\%$ increased activity relative to styrene (observed activity $\sim 212 \text{ mU mg}^{-1}$) was determined indicating a clear *E*-selectivity of the enzyme. It is especially noteworthy that *GrStyA* shows an opposite behavior in the relative activity toward *E*- and *Z*- β -methylstyrene, being more active in the conversion of the *Z*-substrate.

For *GrStyA*, *Z*- β -methylstyrene, β,β -dimethylstyrene and 1,2-dihydronaphthalene were found to show the same or higher enzyme activity than toward styrene. Interestingly, the same compounds that contain the previously mentioned residue in *Z*-position cause a decreased epoxidation activity in *GnIndA*. In addition, for *GrStyA* a reduced activity for *E*- β -methylstyrene was observed which indicates an overall *Z*-selectivity. Furthermore, *GrStyA* converts 1,2-dihydronaphthalene at a comparable rate than styrene while 1-phenyl-1-cyclohexene is converted significantly slower ($7 \pm 1\%$). Thus, *GrStyA* was found to be *Z*-selective.

In general, *GrStyA* catalyzed the epoxidation of all tested substrates and overall, a lesser reduction in activity was observed for most of the substrates. Nevertheless, the actual activity of *GnIndA* is still higher than of *GrStyA* for most tested substrates.

For substrates with ether residues at the aromatic ring, a substitution-specific decrease in activity was observed for both enzymes while the relative product formation was slightly higher for *GrStyA*. Interestingly, the position of the ether moiety correlates similarly with the activity decrease: A methoxy group in *meta*-position was accepted best by both enzymes while the same substituent in *para*-position caused the lowest conversion rate, if converted at all, for both enzymes. These position-specific correlations in enzymatic activity indicate a similar substrate binding at the aromatic ring while the

recognition at the reactive double bond was found to be different due to clear isomer preferences for the enzymes (*GrStyA*: Z-selective, *GrIndA* E-selective).

In addition to the substrate spectrum, the conversion of the standard substrate styrene to styrene oxide by both enzymes was investigated in a higher resolved time scale (Figure 4). *GnIndA* reached a plateau in product amount of 0.70 ± 0.03 mM styrene oxide (35.0% conversion) after 30 min while *GrStyA* produced a maximal amount of 0.47 ± 0.04 mM styrene oxide (23.5% conversion) after 80 min. Further investigations showed that *GrStyA* is stable under the reaction conditions and the cosubstrate limits the reaction, although a five-fold excess of BNAH was supplied (Figure S3). The enzymes used most of the supplied BNAH to produce hydrogen peroxide instead of performing the epoxidation of the substrate. It can be estimated that *GnIndA* has an uncoupling rate of 86% while *GrStyA* shows 91% uncoupling. This uncoupling effect was also described for other enzymes, is typically influenced by the type of electron donor, and was reported for NAD(P)H-mimics before [31–33]. Nevertheless, this obvious drawback of BNAH can be overcompensated by continuous addition of the cosubstrate (Figure S3) which is justified by the low price and easy provision of the compound.

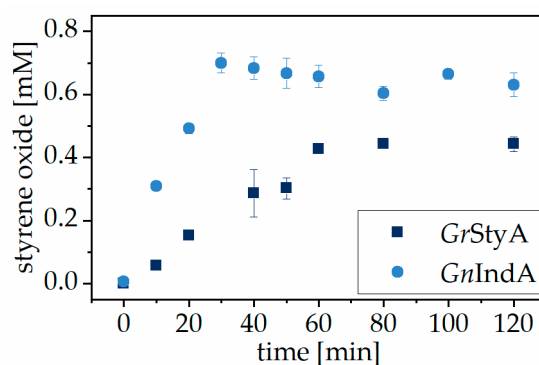


Figure 4. Formation of styrene oxide under optimal conditions (20 mM Tris-HCl pH 7.5, 2 mM styrene, 1 mM dithiothreitol, 5 vol.% glycerol, 20 U/mL catalase and 10 vol.% MeOH for *GnIndA* or 5 vol.% DMSO for *GrStyA*): *GnIndA* produces 0.70 ± 0.03 mM styrene oxide within 30 min (35.0% conversion) while *GrStyA* produced a maximal amount of 0.47 ± 0.04 mM styrene oxide after 80 min (23.5% conversion).

2.3. In Silico Analysis

Because we found the IMO *GnIndA* from *Gemmobacter nectarophilus* DSM15620 to be active even in the presence of substantial amounts of organic solvents while the SMO *GrStyA* from *Gordonia rubripertincta* CWB2 was not, we focused on sequential and structural differences of the enzymes to explain the observed behavior. For this, the structure of the SMO *PpStyA* from *Pseudomonas putida* S12 (PDB accession: 3IHM) was used as template since it is the only known SMO structure so far [34]. Sharing 60% sequence identity with *GrStyA* and 29% with *GnIndA*, *PpStyA* was used to create valid models using the software Modeler 9.23 without the need for further optimization (Figure S4) [35,36].

The *PpStyA* structure was subjected to the FireProt and HotSpot Wizard webserver which highlight so-called hot spot amino acids based on energy minimization and evolutionary mutations [37,38]. Compared to the structural model, these amino acids were found to be located mainly at junctions and interaction surfaces of secondary structure elements which are important for the overall protein stability (Figure 5). In addition, FireProt suggested mutations for these locations to increase the thermostability of the structure (Figure 5a, Table S3). The mutations are further differentiated in energy mutants which result from the artificial energy optimization with random mutagenesis of the structure and in evolutionary mutants which highlight natural occurring mutations in determined hot spots.

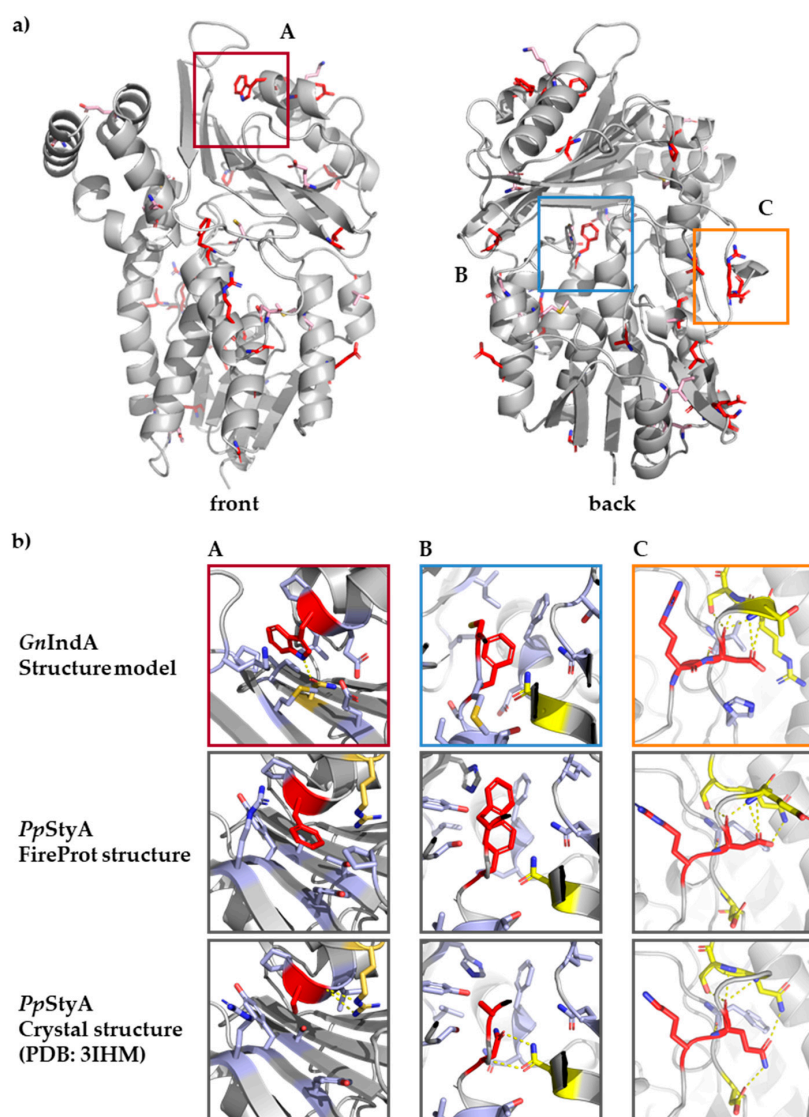


Figure 5. (a) structure model of *GnIndA* calculated with Modeler 9.23 using the SMO structure *PpStyA* from *Pseudomonas putida* S12 (PDB: 3IHM) as template. Amino acids targeted by the FireProt webserver on the template structure are highlighted in the *GnIndA* model: red if mutated, pink if functionally different mutation. (b) Magnification of three structural hot spot regions of the *GnIndA* structure model (top), as highlighted in (a), in comparison with the altered structure (middle) and the template crystal structure (bottom). Color code: red: altered amino acid, yellow: amino acid with directional interaction, blue: amino acid with non-directional interaction and surrounding amino acids. **A:** S249 does not cause hydrophobic interaction with the β -sheet amino acids. The S249F mutation increases the interaction between both secondary structure elements. In the *GnIndA* model, W251 causes hydrophobic interactions as well but additionally rigidifies the structure by a hydrogen bond to N192 of the β -sheet below. **B:** In the *PpStyA* structure, two helices are connected by hydrogen bonds between N51 (red) and N309 while A49 contributes little to the hydrophobic interactions in this central interaction point of three α -helices. By means of FireProt, stronger interactions are achieved by the double mutation A49F/N51F ($\Delta\Delta G = -4.4 \text{ kJ mol}^{-1}$). The *GnIndA* model already contains F50 while C48 contributes more to the hydrophobic interactions than A49 in the *PpStyA* structure. **C:** The mutation Q155D leads to an alternative hydrogen bond network forcing a more rigid α -helical structure while the tightness of the hydration shell is strengthened due to a charge increase by the K154R mutation.

Energy mutation simulations caused in most cases the introduction of large hydrophobic amino acids while the evolutionary mutations are more diverse, albeit expressed in less extreme structural

or functional amino acid exchanges (Table S3). Thus, evolutionary mutations strengthened mainly existing interactions by different mechanisms: through an increase of hydrophobic interactions (e.g., S249F or A49F and N51F, Figure 5bA,B), an introduction of electrostatic interactions (e.g., Q155D, Figure 5bC), an increase of rigidity (e.g., N285P, not shown) or through the variation of charges to increase the tightness of the hydration shell (e.g., K154R, Figure 5bC).

As mentioned before, most of the suggested mutations for *PpStyA* were found at interaction surfaces of secondary structure elements. As an example, S249 is located in the *PpStyA* structure at the tip of the interaction site of the upper helix with the β -sheet below and does not contribute to any hydrophobic interaction with the surrounding amino acids (Figure 5bA). To increase the interaction between both secondary structure elements and prevent unfolding at this position, the replacement of serine by a phenylalanine (S249F) was suggested by FireProt. In the *GnIndA* model, tryptophan (W251) was found in this position which allowed not only increased hydrophobic interactions but additionally rigidifies the structure by a hydrogen bond to N192 of the β -sheet. This and further examples (Figure 5bB,C) highlight that mutations suggested by the FireProt and HotSpot Wizard webserver which are found in the native *GnIndA* sequence fulfill the same purpose with similar contributions to the overall protein stability. Based on these data, we state that the presence of mutations in the *PpStyA* structure suggested by FireProt which are found in the protein sequence of interest correlate with an increased thermo- and solvent stability of the protein as well.

For quantification of the effects, a multiple sequence alignment of *PpStyA* with *GnIndA* together with eight closest related IMOs and *GrStyA* together with 12 related SMOs revealed that half of the suggested mutations for the *PpStyA* structure were naturally present in the *GnIndA* sequence (18 out of 36, Figure S5). Except for one single mutation (Y328F), all evolutionary mutations are present in the *GnIndA* sequence (17 of 18, Table S3). In the *PpStyA* structure, these mutations cause a predicted difference in thermostability of $\Delta\Delta G = -21.5 \text{ kJ mol}^{-1}$. From the suggested energy mutations, only a single mutation was found in the *GnIndA* sequence (A251Y) which contributes to structural stability of $\Delta\Delta G = -12.1 \text{ kJ mol}^{-1}$ in the *PpStyA* structure optimized by FireProt. However, in addition, three correlating residues were found in the *GnIndA* sequence (C49, V226 and W249) which have the same functionalities than the suggested mutations, so that they probably contribute similarly to improved structural stability.

In contrast, native *GrStyA* contains only 19% of the mutations suggested by FireProt (7 out of 36). These variations should still result in an increased stability compared to native *PpStyA* ($\Delta\Delta G = -10.2 \text{ kJ mol}^{-1}$). Still, *GnIndA* can be expected to have a higher stability regarding elevated temperatures which will in last consequence correlate with the enhanced tolerance toward organic solvents.

3. Discussion

Two flavin containing monooxygenases, the SMO *GrStyA* and the IMO *GnIndA*, were probed for their applicability in the stereoselective epoxidation of styrene and eight differently substituted derivatives. Their relative activity and their tolerance toward the varied substitution patterns differed significantly, equally their tolerance toward organic solvents in reaction scenarios relevant for a potential industrial application of these enzymes. The herein presented data give a highly differential picture of these interesting biocatalysts worthy of more in-depth investigation.

While we observed a difference in oxygenation activity for flavin-based two-component monooxygenases in previous studies [11], an in-depth screening of substrate-, cosubstrate- and cosolvent-dependent reactivity has not been reported so far. The conversion of styrene derivatives with a hydrophobic substitution pattern was confirmed for both enzymes under investigation. While *GrStyA* shows an overall broader substrate spectrum, a generally higher activity was observed for *GnIndA* in most cases.

The major difference between both enzymes is their altered product formation rate in the presence of organic solvents. For *GnIndA*, a constant product amount was detected in presence of most tested solvents up to a concentration of 15 vol.%. Furthermore, in presence of 25 vol.% methanol, 43%

residual styrene oxide production was observed and the addition of 5 vol.% THF resulted in the highest increase in product amount for all solvents and concentrations tested. In contrast, addition of 10 vol.% cosolvent resulted in significantly decreased product formation when *GrStyA* was used as biocatalyst for all solvents except for DMSO and ethanol. For those, a product amount above 80% relative to unsubstituted styrene was still detected.

To explain the observed differences with respect to supplied solvents, structural calculations were performed. The styrene monooxygenase *PpStyA* from *Pseudomonas putida* S12 (PDB accession: 3IHM) was used in our in silico approach since it is the only reported SMO structure so far (Figure S5). By means of FireProt one can predict potential mutations to reach a more (thermo)stable enzyme. This tool can be supported by the HotSpot Wizard server, predicting potential sites to improve overall protein stability. Solvent- and thermostability often go hand in hand and thus we employed these tools together to rationalize our findings. The results revealed that *GnIndA* contains half of the suggested mutations (18 out of 36, FireProt) and shows functionally altered amino acids in highlighted stability hot spots in 86% of all cases (36 out of 42, HotSpot Wizard). By analysis of these amino acids in context of the protein structure, we showed a functional conservation in the model for *GnIndA* for these highlighted amino acids and demonstrated a structure-sequence dependency. Based on these data, we deduce higher stabilities for proteins that intrinsically contain the in silico suggested mutations in their native sequence. *GrStyA* naturally contains only 19% of the FireProt (7 out of 36) and 52% HotSpot Wizard sites (22 out of 42). These results indicate a higher thermostability of *GnIndA* which correlates with the observed increased tolerance toward organic solvents.

The IMO *GnIndA* produces a remarkably high styrene oxide amount in presence of several water-miscible solvents. In addition, the enzyme contains a unique set of mutations among related IMO which correlate with structural changes suggested by the FireProt webserver in order to generate a more stable protein. Combining both facts, we consider *GnIndA* to be the first solvent-tolerant IMO.

Interestingly, seven of the 18 crucial amino acids of *GnIndA* that are altered in comparison to *PpStyA* are conserved in the other nine aligned IMOs while no such conservation was found for the aligned SMO sequences (Table S3). In general, the chances to find solvent tolerance can be estimated to be higher for IMOs than SMOs. Further investigations on sequence level will show if other enzymes with higher stability than *GnIndA* exist in the subfamily.

4. Materials and Methods

Chemicals, substrates, and solvents were purchased from commercial supplier (Sigma Aldrich, Darmstadt, Germany; TCI Europe, Zwijndrecht, Belgium; and VWR, Darmstadt, Germany) in the highest purity available. BNAH was synthesized as described previously [39].

Enzyme production and purification. The respective genes for *GrStyA* (ASR05591) and *GnIndA* (WP_028028710) were each cloned by NotI and NdeI sites into a pET16bp vector under the control of a T7-promotor (1 mM IPTG for induction) using standard molecular biology tools [11]. The genes were then expressed heterologously in *E. coli* BL21 (DE3), growing by overnight shaking in baffled flasks in lysogeny broth (LB) medium (10 g L⁻¹ tryptone, 5 g L⁻¹ yeast extract, 10 g L⁻¹ NaCl) at 37 °C. The cells were harvested by centrifugation and lysed using ultrasonication. The proteins were purified from cell free crude extract by nickel affinity chromatography and stored at −20 °C in 50 mM Tris-HCl buffer, pH 7.5, containing 50% glycerol and 1 mM dithiothreitol. Purity of the enzymes was verified by SDS-PAGE.

Protein quantification. Protein concentrations were determined by the Bradford method [40] using Bio-Rad protein assay reagent (#5000006). Bovine serum albumin (Sigma Aldrich, Darmstadt, Germany) served as a reference protein.

Biotransformation standard conditions. The enzymatic reaction was performed in a total volume of 200 µL in a 1.5 mL glass vial according to earlier descriptions [12,22,26]. Under standard conditions, the solution contained 20 mM Tris-HCl pH 7.5, 50 µM FAD, 10 mM BNAH, 1 mM dithiothreitol, 5 vol.% glycerol, 20 U/mL catalase from bovine liver and 10 vol.% methanol for *GnIndA* or 5 vol.% dimethyl

sulfoxide for GrStyA. An appropriate amount of enzyme (3.0 μ M GrStyA, 2.7 μ M GnIndA) was added and the solution was preheated to 30 °C for ten minutes at 750 rpm shaking before the reaction was started by addition of 2 mM substrate. Samples were taken immediately after substrate addition and after 2 h reaction time. If not indicated differently, styrene was used as standard substrate for all comparative studies.

Cofactor, cosubstrate and cosolvent optimization. The enzymatic reaction was performed as described above, but the concentration of the investigated compound was changed according to the following concentrations. The minimal required amount of dissolved FAD cofactor was identified by applying a concentration range from 0 to 100 μ M FAD. For determination of the optimal cosubstrate concentration a range between 5 and 25 mM BNAH was applied in the standard conditions. To determine the optimal cosolvent and its concentration for GnIndA, 5 to 25 vol.% of a variety of different water-miscible solvents were tested in 5 vol.% increments. For GrStyA, 10 vol.% concentrations were tested. All conditions were compared by the amount of produced styrene oxide after 2 h reaction time normalized to the produced amount under the above-described standard conditions.

Initial enzyme activity. The enzymatic reaction for all tested substrates was performed in triplicates under the standard conditions described above. The volume of the reaction increased to 250 μ L and 30 μ L samples were taken after 5, 10, 20 and 30 min of reaction time and analyzed by HPLC. The initial activity of the respective enzymes toward a certain substrate was determined relative to styrene by comparing the slope of the linear part in product formation to the slope observed for styrene as substrate.

Time-dependent product formation. The enzymatic reaction was performed under the standard conditions described above in a twelve-fold multiplicate. Within the first hour, samples were taken every ten minutes and then every 20 minutes, from three random vials to a maximum of three samples per vial to avoid effects caused by the loss of volume during the experiment.

Synthesis of product standards. For determination of the HPLC retention times for the enzymatic products, the following three reactions were compared: First, the purchased substrate standard was measured. Through addition of excess *meta*-chloroperoxybenzoic acid to the substrate containing measurement vial in solid form, the respective epoxide was synthesized chemically in situ, which resulted in the observation of a second peak corresponding to a more polar substance. The further addition of water containing 0.1 vol.% trifluoroacetic acid led to disappearance of the epoxide peak and to detection of an even more polar compound, which is assigned to the respective diol. The procedure was validated for styrene, for which commercial standards of styrene oxide and 1-phenylethane-1,2-diol were available.

HPLC analysis. The produced epoxide amount was quantified by HPLC measurements (Thermo Scientific, Oberhausen, Germany) using an isocratic method at 60 vol.% acetonitrile in water on a Knauer Eurospher 100-5 C18 Vertex plus column (size: 125 \times 4 mm, pore size: 100 Å, particle size: 5 μ m; Knauer, Berlin, Germany) as stationary phase. Compounds were detected by UV/vis absorbance at 214 nm. The system was calibrated using commercially available styrene and racemic styrene oxide.

GC-FID analysis. Chiral GC-FID analysis was used to determine the enantiomeric excess of the product. For this, the enzymatically produced epoxidation product was extracted from the reaction solution with one volume ethyl acetate. The organic phase was dried over anhydrous magnesium sulfate and analyzed using a Macherey-Nagel Hydrodex β -6TBDM column (length: 50 m, inner diameter: 0.25 mm; Macherey-Nagel, Düren, Germany) under isothermal conditions at 100 °C by means of GC-FID (Shimadzu, Duisburg, Germany). The calibration was performed using commercially available styrene and (S)-styrene oxide.

In silico calculation of hot spot amino acids. The only known structure of the styrene monooxygenase PpStyA from *Pseudomonas putida* S12 (PDB accession number: 3IHM) was used to calculate crucial amino acids for protein stability using the HotSpot Wizard [38] and FireProt [37] webserver. The results were compared by a multiple sequence alignment of 15 SMOs closely related to GrStyA and 10 IMOs related to GnIndA. The alignment was calculated using Mega X (10.1.5) [41]. From the absence or

presence of suggested mutations in each sequence in comparison to *PpStyA*, conclusions about the overall stability were drawn.

Homology modeling. The structural model for *GnIndA* was constructed using Modeler 9.23 [35]. The structure of *PpStyA* from *Pseudomonas putida* S12 (PDB accession number: 3IHM) served as template together with the structure files obtained from the FireProt results (see above) as template.

5. Conclusions

To sum up, we successfully optimized the reaction conditions for two flavin containing two-component monooxygenases regarding the conversion of large hydrophobic substrates. The intriguingly different preference for *E*- respective *Z*-enantiomeric substrates by *GrIndA* resp. *GrStyA* bears a high potential for industrial applications, e.g., when it comes to enantiomer separation in complex mixtures.

Furthermore, *GnIndA* was found to be remarkably tolerant toward nine tested organic solvents. This can be explained by beneficial mutations in crucial residues matching the predicted increased stability based on in silico calculations. In addition, these suggested mutations can be used to construct the most stable protein sequence for a targeted search for even more stable IMOs, but at the same time give valuable insight into potential stabilization strategies also for SMOs. Respectively, we could simplify and conclude that IMOs are more stable biocatalysts.

Supplementary Materials: The following are available online at <http://www.mdpi.com/2073-4344/10/5/568/s1>, Figure S1. SDS gel of the protein production, Table S1. Organic solvents used to optimize the enzymatic epoxidation of styrene, Figure S2. Concentration of 1-phenyl-1-cyclohexane in aqueous solution in presence of different organic cosolvents, Table S2. Enantiomeric excess of (*S*)-styrene oxide produced by *GnIndA* in presence of selected organic solvents, Figure S3. Continuously fed biotransformation of styrene to styrene oxide by *GrStyA*, Figure S4. Results of the quality check of the structural *GnIndA* model, Figure S5. Multiple sequence alignment of *GnIndA*, *GrStyA* and *PpStyA* with 22 related SMOs and IMOs, Table S3. FireProt mutations in comparison with their abundance among IMOs and SMOs.

Author Contributions: Supervision: D.T., conceptualization: D.T., U.-P.A. Investigations: D.E., J.M., Software: D.E., writing—original draft: D.T., D.E. writing—review and editing: C.M., U.-P.A. All authors have read and agreed to the published version of the manuscript.

Funding: D.E. received funding from the Deutsche Bundesstiftung Umwelt (PhD scholarship). The project was supported by the Deutsche Forschungsgemeinschaft (RTG 2341 MiCon). C.M., and D.T. were funded by the Federal Ministry for Innovation, Science and Research of North Rhine–Westphalia (PtJ-TRI/1411ng006—ChemBioCat). U.-P.A. is grateful for financial support from the Deutsche Forschungsgemeinschaft (Emmy Noether grant AP242/2-1) and the Fraunhofer Internal Programs under Grant No. Attract 097-602175.

Acknowledgments: We thank Thomas Heine (TU Bergakademie Freiberg) for fruitful discussions and support during the experimental phase.

Conflicts of Interest: The authors declare no conflict of interest.

References

1. Copley, S.D. Evolution of a metabolic pathway for degradation of a toxic xenobiotic: The patchwork approach. *Trends Biochem. Sci.* **2000**, *25*, 261–265. [CrossRef]
2. Heine, T.; Zimmerling, J.; Ballmann, A.; Kleeberg, S.B.; Rückert, C.; Busche, T.; Winkler, A.; Kalinowski, J.; Poetsch, A.; Scholtissek, A.; et al. On the enigma of glutathione-dependent styrene degradation in *Gordonia rubripertincta* CWB2. *Appl. Environ. Microbiol.* **2018**, *84*, e00154–18. [CrossRef] [PubMed]
3. Tischler, D. *Microbial Styrene Degradation*; Springer International Publishing: Cham, Switzerland, 2015; ISBN 978-3-319-24860-8.
4. Furnes, B.; Schlenk, D. Evaluation of xenobiotic *N*- and *S*-oxidation by variant flavin-containing monooxygenase 1 (FMO1) enzymes. *Toxicol. Sci.* **2004**, *78*, 196–203. [CrossRef] [PubMed]
5. Lin, G.-H.; Chen, H.-P.; Shu, H.-Y. Detoxification of indole by an indole-induced flavoprotein oxygenase from *Acinetobacter baumannii*. *PLoS ONE* **2015**, *10*, e0138798. [CrossRef] [PubMed]
6. Montersino, S.; Tischler, D.; Gassner, G.T.; van Berkel, W.J.H. Catalytic and structural features of flavoprotein hydroxylases and epoxidases. *Adv. Synth. Catal.* **2011**, *353*, 2301–2319. [CrossRef]

7. Huijbers, M.M.E.; Montersino, S.; Westphal, A.H.; Tischler, D.; van Berkel, W.J.H. Flavin dependent monooxygenases. *Arch. Biochem. Biophys.* **2014**, *544*, 2–17. [[CrossRef](#)] [[PubMed](#)]
8. Hollmann, F.; Lin, P.-C.; Witholt, B.; Schmid, A. Stereospecific biocatalytic epoxidation: The first example of direct regeneration of a FAD-dependent monooxygenase for catalysis. *J. Am. Chem. Soc.* **2003**, *125*, 8209–8217. [[CrossRef](#)]
9. Lin, H.; Liu, Y.; Wu, Z.-L. Asymmetric epoxidation of styrene derivatives by styrene monooxygenase from *Pseudomonas* sp. LQ26: Effects of α - and β -substituents. *Tetrahedron Asymmetry* **2011**, *22*, 134–137. [[CrossRef](#)]
10. Lin, H.; Qiao, J.; Liu, Y.; Wu, Z.-L. Styrene monooxygenase from *Pseudomonas* sp. LQ26 catalyzes the asymmetric epoxidation of both conjugated and unconjugated alkenes. *J. Mol. Catal. B Enzymatic* **2010**, *67*, 236–241. [[CrossRef](#)]
11. Heine, T.; Scholtissek, A.; Hofmann, S.; Koch, R.; Tischler, D. Accessing enantiopure epoxides and sulfoxides: Related flavin-dependent monooxygenases provide reversed enantioselectivity. *ChemCatChem* **2020**, *12*, 199–209. [[CrossRef](#)]
12. Tischler, D.; Schwabe, R.; Siegel, L.; Joffroy, K.; Kaschabek, S.R.; Scholtissek, A.; Heine, T. VpStyA1/VpStyA2B of *Variovorax paradoxus* EPS: An aryl alkyl sulfoxidase rather than a styrene epoxidizing monooxygenase. *Molecules* **2018**, *23*, 809. [[CrossRef](#)] [[PubMed](#)]
13. Hwang, S.; Choi, C.Y.; Lee, E.Y. Bio- and chemo-catalytic preparations of chiral epoxides. *J. Ind. Eng. Chem.* **2010**, *16*, 1–6. [[CrossRef](#)]
14. Breuer, M.; Ditrach, K.; Habicher, T.; Hauer, B.; Kessler, M.; Stürmer, R.; Zelinski, T. Industrial methods for the production of optically active intermediates. *Angew. Chem. Int. Ed. Engl.* **2004**, *43*, 788–824. [[CrossRef](#)] [[PubMed](#)]
15. Lin, H.; Liu, J.-Y.; Wang, H.-B.; Ahmed, A.A.Q.; Wu, Z.-L. Biocatalysis as an alternative for the production of chiral epoxides: A comparative review. *J. Mol. Catal. B Enzymatic* **2011**, *72*, 77–89. [[CrossRef](#)]
16. Torres Pazmiño, D.E.; Winkler, M.; Glieder, A.; Fraaije, M.W. Monooxygenases as biocatalysts: Classification, mechanistic aspects and biotechnological applications. *J. Biotechnol.* **2010**, *146*, 9–24. [[CrossRef](#)]
17. De Vries, E.J.; Janssen, D.B. Biocatalytic conversion of epoxides. *Curr. Opin. Biotechnol.* **2003**, *14*, 414–420. [[CrossRef](#)]
18. Panke, S.; Held, M.; Wubbolts, M.G.; Witholt, B.; Schmid, A. Pilot-scale production of (S)-styrene oxide from styrene by recombinant *Escherichia coli* synthesizing styrene monooxygenase. *Biotechnol. Bioeng.* **2002**, *80*, 33–41. [[CrossRef](#)]
19. Gao, P.; Wu, S.; Praveen, P.; Loh, K.-C.; Li, Z. Enhancing productivity for cascade biotransformation of styrene to (S)-vicinal diol with biphasic system in hollow fiber membrane bioreactor. *Appl. Microbiol. Biotechnol.* **2017**, *101*, 1857–1868. [[CrossRef](#)]
20. Schmid, A.; Hofstetter, K.; Feiten, H.-J.; Hollmann, F.; Witholt, B. Integrated biocatalytic synthesis on gram scale: The highly enantioselective preparation of chiral oxiranes with styrene monooxygenase. *Adv. Synth. Catal.* **2001**, *2001*, 343.
21. Mascotti, M.L.; Juri Ayub, M.; Furnham, N.; Thornton, J.M.; Laskowski, R.A. Chopping and changing: The evolution of the flavin-dependent monooxygenases. *J. Mol. Biol.* **2016**, *428*, 3131–3146. [[CrossRef](#)]
22. Tischler, D.; Eulberg, D.; Lakner, S.; Kaschabek, S.R.; van Berkel, W.J.H.; Schlömann, M. Identification of a novel self-sufficient styrene monooxygenase from *Rhodococcus opacus* 1CP. *J. Bacteriol.* **2009**, *191*, 4996–5009. [[CrossRef](#)] [[PubMed](#)]
23. Tischler, D.; Gröning, J.A.D.; Kaschabek, S.R.; Schlömann, M. One-component styrene monooxygenases: An evolutionary view on a rare class of flavoproteins. *Appl. Biochem. Biotechnol.* **2012**, *167*, 931–944. [[CrossRef](#)] [[PubMed](#)]
24. Zhang, W.; Hollmann, F. Nonconventional regeneration of redox enzymes—A practical approach for organic synthesis? *Chem. Commun.* **2018**, *54*, 7281–7289. [[CrossRef](#)] [[PubMed](#)]
25. Tischler, D.; Schlömann, M.; van Berkel, W.J.H.; Gassner, G.T. FAD C(4a)-hydroxide stabilized in a naturally fused styrene monooxygenase. *FEBS Lett.* **2013**, *587*, 3848–3852. [[CrossRef](#)] [[PubMed](#)]
26. Paul, C.E.; Tischler, D.; Riedel, A.; Heine, T.; Itoh, N.; Hollmann, F. Nonenzymatic regeneration of styrene monooxygenase for catalysis. *ACS Catal.* **2015**, *5*, 2961–2965. [[CrossRef](#)]
27. Hollmann, F.; Hofstetter, K.; Habicher, T.; Hauer, B.; Schmid, A. Direct electrochemical regeneration of monooxygenase subunits for biocatalytic asymmetric epoxidation. *J. Am. Chem. Soc.* **2005**, *127*, 6540–6541. [[CrossRef](#)]

28. Hansch, C.; Leo, A.; Hoekman, D. *Hydrophobic, Electronic, and Steric constants*; American Chemical Society: Washington, DC, USA, 1995; ISBN 0841229929.
29. Toda, H.; Imae, R.; Itoh, N. Efficient biocatalysis for the production of enantiopure (S)-epoxides using a styrene monooxygenase (SMO) and *Leifsonia* alcohol dehydrogenase (LSADH) system. *Tetrahedron Asymmetry* **2012**, *23*, 1542–1549. [[CrossRef](#)]
30. Yalkowsky, H.S.; He, Y.; Jain, P. *Handbook of Aqueous Solubility Data*, 2nd ed.; CRC Press: Boca Raton, FL, USA, 2010; ISBN 978-1-4398-0246-5.
31. Morrison, E.; Kantz, A.; Gassner, G.T.; Sazinsky, M.H. Structure and mechanism of styrene monooxygenase reductase: New insight into the FAD-transfer reaction. *Biochemistry* **2013**, *52*, 6063–6075. [[CrossRef](#)]
32. Gassner, G.T. The styrene monooxygenase system. *Meth. Enzymol.* **2019**, *620*, 423–453. [[CrossRef](#)]
33. Massey, V. Activation of molecular oxygen by flavins and flavoproteins. *J. Biol. Chem.* **1994**, *269*, 22459–22462.
34. Ukaegbu, U.E.; Kantz, A.; Beaton, M.; Gassner, G.T.; Rosenzweig, A.C. Structure and ligand binding properties of the epoxidase component of styrene monooxygenase. *Biochemistry* **2010**, *49*, 1678–1688. [[CrossRef](#)] [[PubMed](#)]
35. Webb, B.; Sali, A. Comparative protein structure modeling using MODELLER. *Curr. Protoc. Bioinform.* **2016**, *54*, 5–6. [[CrossRef](#)]
36. Eisenberg, D.; Lüthy, R.; Bowie, J.U. VERIFY3D: Assessment of protein models with three-dimensional profiles. *Methods Enzymol.* **1997**, *277*, 396–404. [[CrossRef](#)] [[PubMed](#)]
37. Musil, M.; Stourac, J.; Bendl, J.; Brezovsky, J.; Prokop, Z.; Zendulka, J.; Martinek, T.; Bednar, D.; Damborsky, J. FireProt: Web server for automated design of thermostable proteins. *Nucleic Acids Res.* **2017**, *45*, W393–W399. [[CrossRef](#)] [[PubMed](#)]
38. Sumbalova, L.; Stourac, J.; Martinek, T.; Bednar, D.; Damborsky, J. HotSpot Wizard 3.0: Web server for automated design of mutations and smart libraries based on sequence input information. *Nucleic Acids Res.* **2018**, *46*, W356–W362. [[CrossRef](#)]
39. Paul, C.E.; Arends, I.W.C.E.; Hollmann, F. Is simpler better? Synthetic nicotinamide cofactor analogues for redox chemistry. *ACS Catal.* **2014**, *4*, 788–797. [[CrossRef](#)]
40. Bradford, M.M. A rapid and sensitive method for the quantitation of microgram quantities of protein utilizing the principle of protein-dye binding. *Anal. Biochem.* **1976**, *72*, 248–254. [[CrossRef](#)]
41. Kumar, S.; Stecher, G.; Li, M.; Knyaz, C.; Tamura, K. MEGA X: Molecular evolutionary genetics analysis across computing platforms. *Mol. Biol. Evol.* **2018**, *35*, 1547–1549. [[CrossRef](#)]



© 2020 by the authors. Licensee MDPI, Basel, Switzerland. This article is an open access article distributed under the terms and conditions of the Creative Commons Attribution (CC BY) license (<http://creativecommons.org/licenses/by/4.0/>).